Journal of Metals, Materials and Minerals, 35(2), e2180, 2025

The influence of aluminium dross residue and coal fly ash on the properties of geopolymers

Haswanee PHUNGPHA[1], Pitak LAORATANAKUL[2], and Benya CHERDHIRUNKORN[1,3,*]

[1] *Division of Materials and Textiles Technology, Faculty of Science and Technology, Thammasat University, Patumthani, 12120, Thailand*
[2] *National Metal and Materials Technology Center (MTEC), National Science and Technology Development Agency (NSTDA), Patumthani, 12120, Thailand*
[3] *Research Unit in Sustainable Materials and Circular Economy, Thammasat University, Patumthani, 12120, Thailand*

***Corresponding author e-mail**: benya@tu.ac.th

Received date:
13 October 2024
Revised date:
4 February 2025
Accepted date:
17 March 2025

Keywords:
Geopolymer;
Aluminium dross residue;
Fly ash

Abstract

In this research, aluminium dross residue (AD) and coal fly ash (FA) were used for the production of geopolymers. The illegal dumping of AD and the high cost for AD waste disposal have been problems for long time in Thailand. Therefore, the feasibility of using AD (0 wt% to 100 wt%) in the geopolymer production had been carried out to find the alternative way to resolve these problems. The alkaline solution of NaOH 7 M and Na_2SiO_3 with the ratio of 1:3 was used for the geopolymerization reaction. It was found that the addition of AD caused the ammonia gas during the process, which resulted in high porosity of the samples. The low compressive strength, low density and low thermal conductivity were observed in the samples with higher AD contents. The results indicated that the sample with 50 wt% AD and 50 wt% FA gave the reasonable properties for lightweight concrete block with the density of 1.56 $g\cdot cm^{-3}$, the compressive strength of 6.32 MPa, and the water absorption of 4.26%. In addition, the phase structure, microstructure and the structure change of the geopolymer samples were investigated using XRD, SEM and FTIR techniques, respectively.

1. Introduction

Environmental problem and global warming are the importance issues that need to be solved. The greenhouse gases emitted from many industrial and agricultural processes should be controlled and reduced in order to achieve the sustainable development goals. Cement production is one of the high carbon dioxides (CO_2) emission and high energy consumption process. The production of 1000 kg of cement emits approximately 1000 kg of CO_2. The calcination of cement occurs at temperature above 1400°C [1]. Although cement is an importance binding material for concrete which is the most widely used material in construction due to its high strength and good weather resistance, it causes seriously high CO_2 emission. Thus, the development of alternative binding materials has been intensively studied. Numbers of research works reported about a new material called “Geopolymer” which is possibly one of the alternative materials that can be used instead of cement [2-4]. The production of geopolymer emits much lower CO_2 and uses much lower energy comparing to cement production. Geopolymer is an inorganic polymer with the amorphous structure. High SiO_2 and Al_2O_3 containing materials are required for raw materials in the production of geopolymer. The alkaline solutions such as KOH, NaOH and Na_2SiO_3 were used for the geopolymerization reaction [5]. Geopolymer can be simply produced at room temperature without any complicated process. Various natural clay, industrial and agricultural wastes such as metakaolin, fly ash, blast furnace slag, aluminium dross, rice husk ash and bagasse ash, contain high amount of SiO_2 and Al_2O_3, so they can be used as raw materials for geopolymer production [6].

Numbers of research works on fly ash-based geopolymers have been carried out [7-9]. The fly ash-based geopolymers are high strength materials which could be used substitute for cement. In this research, fly ash from the Mae Moh coal power plant, Lampang, Thailand was used as one of raw materials. Coal fly ash is waste from coal combustion process. After grinding and burning coal to get the heat for the boiler, two types of coal ashes are fly ash (fine dust trapped at the top of furnace) and bottom ash (large size of ash at the bottom of the furnace). Both fly ash and bottom ash have similar composition but different in size. They contain high amount of silica (SiO_2), alumina (Al_2O_3) and calcium oxide (CaO). N. Toobpeng *et al.* reported that the Mae Moh’s fly ash contained 27.6 wt% SiO_2 16.40 wt% Al_2O_3 and quite high lime with 27.2 wt% CaO [7]. Thus, it is a good source for SiO_2 and Al_2O_3 which is suitable for geopolymer production. L. ZHANG *et al.* produced geopolymer materials from decomposed granite waste and fly ash. The higher fly ash content and elevated curing temperature gave rise to the high compressive strength [8]. M. H. Ashfaq *et al.* produced geopolymers concrete using 60 wt% to 90 wt% of fly ash and metakaolin as raw materials and varied the NaOH concentration (12 M, 14 M and 16 M). The geopolymer with 70 wt% of fly ash with NaOH 14 M had the highest strength [9].

In addition, there have been many research works on the green materials with the environmentally friendly purpose. Many waste materials have been selected for the production of green materials, for example, blast furnace slag [6] and aluminium dross [10-12]. The blast furnace slag was used as a raw material for geopolymers [13-14]. The blast furnace slag gave both high strength and high corrosion resistance to geopolymer products. Small amount of aluminium dross

DOI:10.55713/jmmm.v35i2.2180

can be used in the production of concrete and porous mullite ceramic due to the strong reaction of aluminium dross with water. There have been limited numbers of research works on the use of high amount of aluminium dross residue (AD) for geopolymer production. Thus, this research work was carried out in order to investigate the use of AD incorporating with FA for geopolymer production.

Aluminium dross is a byproduct of the aluminium melting process. Aluminium metal can be extracted (recycled) from the aluminium dross after some separation steps. The large heavy lumps with high aluminium metal content are separated out for the recycle process. The small light particles with low aluminium metal content (AD) are screened and collected at the end of the separation process. In Thailand, AD is considered to be a toxic waste because it contains AlN that can react with water and release unpleasant smell of ammonia gas. Inhalation of ammonia gas can cause respiratory issues such as coughing, shortness of breath, and chest pain. Ammonia gas can cause severe irritation and burns to the skin and eyes. In addition, ammonia can react with other compounds in the environment, contributing to air and water pollution [15].

P. Puksisuwan *et al.* [12] had studied on the use of AD as one of the raw materials for geopolymer using low liquid/solid ratio (0.25) in order to suppress the ammonia gas. The pressing process was employed for the forming process. The sample with 50 wt% AD and 50% bagasse ash (BA) gave the highest strength.

P. Puksisuwan *et al.* [12] reported that AD contained 10 wt% of SiO_2 and 66.5% of Al_2O_3, so it could be use incorporate with other wastes with contain higher silica (SiO_2) for the production of geopolymers. In our present work, fly ash was used as another part of raw materials due to its high SiO_2 content. Although the L/S ratio of 0.25 was used in the previous work in order to suppress the ammonia smell [12], the pressing machine might not be available in some place. Thus, in this work the L/S ratio of 0.5 was used to prepare slurry for casting process which is a easier and cheaper process. The mixed alkaline solution of 7 M NaOH and Na_2SiO_3 with the ratio of 1:3 was used for the geopolymerization reaction. The setting time was obtained by VICAT. The bulk density, % porosity and the %water absorption of the samples were determined. The compressive strength test was carried out using Universal testing machine. The phase structure, the chemical structure and the microstructure of the geopolymer samples were observed using XRD, FTIR and SEM techniques, respectively.

2. Materials and experimental

2.1 Materials

In this study, the main raw materials for geopolymer preparation were AD from Top Five Manufactory Co., Ltd., Chachengsao, Thailand and FA from Mae Moh power plant, Lampang, Thailand. Analysis of the chemical composition, phase structure and chemical structure of AD and FA was performed using X-ray fluorescence (XRF, Bruker S6 JAGUAR), X-ray diffraction (XRD, Bruker D2 PHASER) and Fourier transform infrared spectroscopy (FTIR, Shimadzu IR Spirite, QATR-S), respectively.

The chemical composition of AD and FA analyzed by XRF technique are shown in Table 1. The main constituents of the AD were Al_2O_3 (64.1 wt%), SiO_2 (6.3 wt%), MgO (7.9 wt%) and Na_2O (3 wt%). On the other hand, fly ash consisted of higher SiO_2 content (26.8 wt%) with other oxides such as Al_2O_3 (15.2 wt%), Fe_2O_3 (14.5 wt%) and quite high CaO (21.5 wt%).

The XRD patterns of AD and FA shown in Figure 1 indicates that major phases found in AD are SiO_2, AlN, Al_2O_3, Al and $3Al_2O_3{\cdot}SiO_2$. The minor phases in AD are $CaCO_3$, $MgAl_2O_4$ and KCl. For the XRD pattern of FA, the main phases are SiO_2, Al_2O_3, Fe_2O_3, $3Al_2O_3{\cdot}SiO_2$ and CaO.

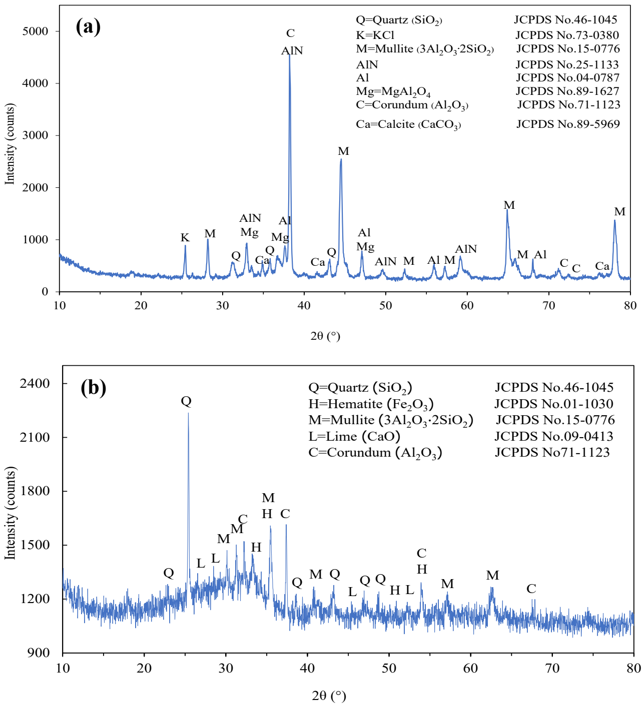

Figure 1. Phase structure of raw materials by XRD (a) aluminium dross residue, and (b) fly ash.

Table 1. Chemical composition of aluminium dross residue (AD) and fly ash (FA).

Oxide composition	Aluminium dross residue (AD) [wt%]	Fly ash (FA) [wt%]
SiO_2	6.3	26.8
Al_2O_3	64.1	15.2
Fe_2O_3	1.9	14.5
CaO	1.6	21.6
MgO	7.9	2.1
Na_2O	3	1.7
K_2O	1	1.9
SO_3	0.5	6
Total	86.3	89.8
Loss on ignition	13.7	10.2

Figure 2 represents the FTIR spectrum of AD and FA that shows the presence of different vibrations corresponding to components. The peaks at 1100 cm^{-1}, 900 cm^{-1}, and 450 cm^{-1} belong to Si-O-Si vibration. The peaks at 600 cm^{-1} and 700 cm^{-1} to Si-O-Al vibration. As for the AD, a small peak appears at wave number 450 cm^{-1} by the vibration of Si-O-Si and at the wavenumber 700 cm^{-1} by the vibration of the Si-O-T functional group (T=Al/Si).

2.2 Sample preparation

Aluminium dross residue (AD) was sieved through mesh number 160 (150 µm) to remove large particles. Solid raw materials (AD and FA) were weighted according to the conditions shown in Table 2. The preparation process for geopolymer samples is shown in Figure 3. The solid raw materials were mixed with alkaline solution of 7 M sodium hydroxide solution (purity of NaOH, NaOH 99%, Na_2CO_3 0.5%, NaCl 0.04, Fe_2O_3 0.005%) and sodium silicate solution (Na_2SiO_3, Technical grade : 42-43 Baume). In addition, from the prior experiment on the effect of NaOH/Na_2O_3 ratio (1:1, 1:2, and 1:3) on the setting time, the ratio of 1:1 and 1:2 resulted in the slow reaction and long setting time (more than 60 min). Thus, the suitable ratio of NaOH/Na_2SiO_3 used for all conditions was 1:3 where the setting time is around 40 min. The liquid/solid ratio of 0.5 (by weight) was used for the slurry mixture which can be easily casted into a silicone mould with the size of 2.5 cm × 2.5 cm × 2.5 cm. The samples were cured at room temperature [16] for 7 day, 14 day, and 28 day prior the sample characterization. The geopolymerization reaction continues for many days after mixing. The completion of the reaction depends on amount of each raw material in the mixture [17].

2.3 Characterization

The setting time of geopolymer mixtures were obtained via VICAT method. The bulk density and the water absorption of the 28 day cured samples were measured and calculated as shown in Equation (1-2). The compressive strength of the samples was determined using Universal Testing Machine (Tinius Olsen H50KT) with the loading rate of 5 mm·min^{-1}.

$$\text{Bulk Density} = \frac{\text{M (g)}}{\text{V (cm}^3\text{)}} \qquad (1)$$

M = the weight of the sample (g)
V = the sample volume width × length × height (cm^3)

$$\text{\%Water Absorption} = \frac{W_S - W_D}{W_D} \times 100 \qquad (2)$$

W_S = wet sample weight (g), 24 h soaking time
W_D = dry sample weight (g)

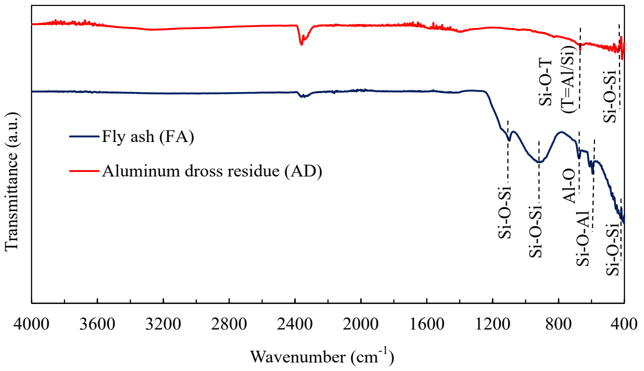

Figure 2. chemical structure of aluminium dross residue (AD) and fly ash (FA) by FTIR.

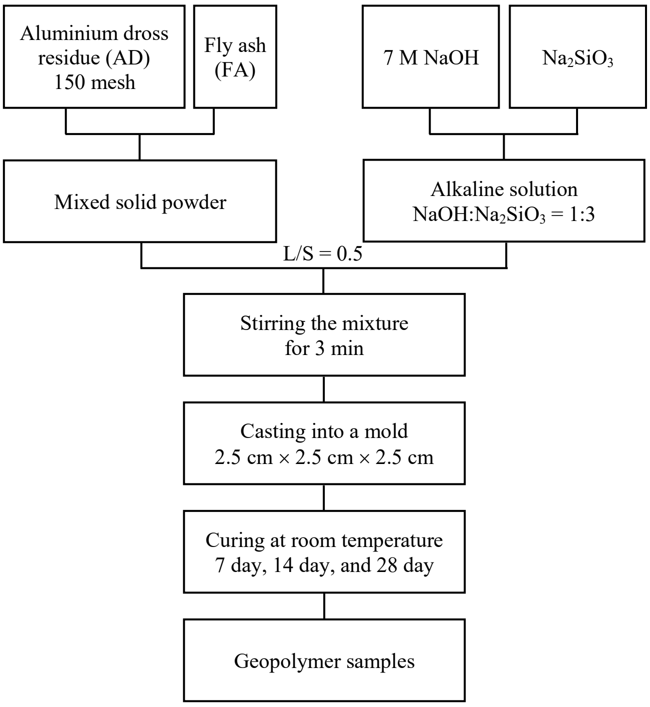

Figure 3. The production of the geopolymer samples.

Table 2. Conditions of the geopolymer samples.

Sample	**Aluminium dross residue (AD) [wt%]**	**Fly ash (FA) [wt%]**
0AD	0	100
10AD	10	90
20AD	20	80
30AD	30	70
40AD	40	60
50AD	50	50
60AD	60	40
70AD	70	30
80AD	80	20
90AD	90	10
100AD	100	0

Phase structures of the ground geopolymer samples were investigated using XRD (X-Ray diffractometer, Bruker/D2 PHASER) operated at a voltage of 30 kV, a current of 10 mA from 2θ of 10° to 80° with the time per step of 0.2 s. The chemical structures of samples were analysed using FTIR techniques, Microstructure of the geopolymer samples were observed using Field emission scanning electron microscope (FE-SEM, JEOL, JSM-7800F).

3. Results and discussion

3.1 Setting time

The setting time of the geopolymer samples shown in Figure 4 was determined using VICAT test apparatus (ASTM C191). The results reveal that the samples with 100% fly ash (0AD) had the fastest setting time. On the other hand, the addition of AD could slow down the setting time, where the 100AD samples took the longest setting time of 26 min.

3.2 Bulk density, true density and porosity

Figure 5 shows that the bulk density of geopolymer samples is in the ranges between 0.93 g·cm^{-3} and 2.06 g·cm^{-3}. The bulk density of the samples decreased with an increase of AD content. The 0AD sample had the highest density of 2.06 g·cm^{-3}, while the 100AD had the lowest density 0.93 g·cm^{-3}. This is due to the releasing of ammonia gas during the geopolymerization reaction. The ammonia gas bubbles were generated when AlN in AD reacted with water, as shown in Equation (4) [18]. The ammonia gas bubbles in the slurry of the raw materials mixture led to the formation of pores in the AD rich samples. After setting, high porosity samples (low bulk density) were formed. The true density obtained using pycnometer method and % porosity are shown in Table 3. The porosity can be calculated via formula (5). Figure 6 shows the different appearance of the samples without AD (0AD) and with various amount of AD (30AD, 50AD, 70AD and 90AD). The higher porosity can be seen in the sample with higher amount of AD.

$$\mathrm{AlN}_{(s)} + 3\mathrm{H_2O}_{(l)} = \mathrm{Al(OH)_3}_{(s)} + \mathrm{NH_3}_{(g)} \qquad (4)$$

$$\%\ \text{Porosity} = \left(1 - \frac{\text{Bulk density}}{\text{True density}}\right) \times 100 \qquad (5)$$

3.3 Water absorption

The results of the water absorption of geopolymers (0AD to 100AD) shown in Figure 7 are consistent with the results of bulk density. The samples with low bulk density and high porosity (higher amount of AD) show the higher water absorption (%). The 100AD sample has the highest water absorption of 19.6%, which exhibits the highest %porosity.

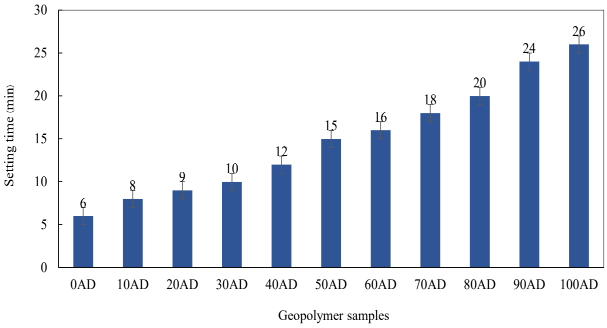

Figure 4. Setting time of geopolymer samples.

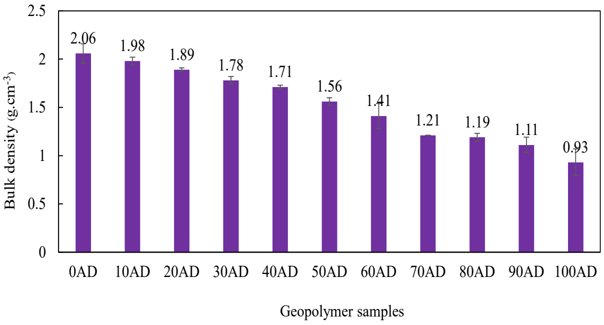

Figure 5. Bulk density of geopolymer samples.

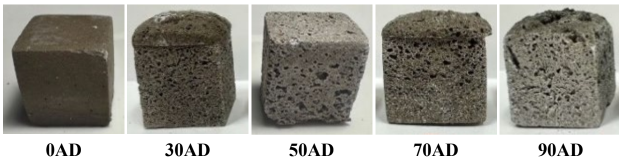
0AD **30AD** **50AD** **70AD** **90AD**

Figure 6. The appearance of Al-dross and fly ash based geopolymers with different AD contents.

Table 3. The true density, bulk density and %porosity of samples.

Sample	True density [g·cm^{-3}]	Bulk density [g·cm^{-3}]	% Porosity
0AD	3.02	2.06	31.79
10AD	2.88	1.98	31.25
20AD	2.85	1.89	33.68
30AD	2.80	1.78	36.43
40AD	2.74	1.71	37.59
50AD	2.69	1.56	42.01
60AD	2.52	1.41	44.05
70AD	2.34	1.21	48.29
80AD	2.26	1.19	47.35
90AD	2.19	1.11	49.32
100AD	1.87	0.93	50.27

3.4 Compressive strength of geopolymers

Compressive strength of the geopolymer samples (0AD to 100AD) after curing for 7 day, 14 day, and 28 day shown in Figure 8. It was found that the compressive strength of all samples increased with the longer curing times. The longer curing period allows the samples to develop a more complete geopolymerization reaction. The 0AD specimens that were cured for 7 day, 14 day, and 28 day had compressive strengths of 15 MPa, 16.5 MPa, and 17.8 MPa, respectively. However, the geopolymer samples with AD showed a reduction in compressive strength. This is due to the higher porosity of the geopolymer structure. The 100AD specimen having the lowest compressive strength of 1.38 MPa after curing for 28 day. However, according to the Thai Industrial Standard (TIS) 2601-2013, the required compressive strength of the lightweight block should not be less than 2 MPa to 5 MPa, the water absorption should be less than 20% and the density should be within the range of 0.5 $g\cdot cm^{-3}$ to 1.6 $g\cdot cm^{-3}$, there were 2 samples (50AD and 60AD) showing the properties within the ranges of standard values. Thus, these samples could be used in the application of lightweight block.

3.5 Phase structure using XRD

From Figure 9, the XRD patterns of the geopolymer samples (0AD-100AD) exhibit broad peaks between 2θ of 20° to 35° indicating the amorphous nature of geopolymer. However, there are peaks of unreacted raw materials remaining, for example, SiO_2 at 2θ of 29° and 42°, Al_2O_3 at 2θ of 35°, 58°, and 42°. Both SiO_2 and Al_2O_3 are abundant in the fly ash. The sample with the highest aluminum dross content (100AD), shows peaks at 2θ of 20° and 63°, indicating the presence of AlN. This aligns with the XRD patterns of raw materials as previously mentioned.

3.6 FTIR : Fourier transform infrared spectroscopy

From the analysis using FTIR technique, it was found that all conditions establish a similar chemical structure as shown in Figure 10. The appearance of spectra at different wavenumber positions of the geopolymer material indicates molecular bonds within the geopolymer. The peak at the wavenumber of 2400 cm^{-1} results from the stretching of the O-H functional group during the production process. When the raw materials undergo the geopolymerization reaction with alkali solutions, there is an increase in water content within the structure and pores of the geopolymer samples, thus a peak at the wavenumber of 3400 cm^{-1} representing water molecules (H-O-H bending) was found. The peak indicating the structural transformation into a geopolymer, caused by the vibration of the T-O-Si functional group (T=Si/Al), is presented at the wavenumber between 900 cm^{-1} to 1100 cm^{-1}. In solid raw material (FA), the asymmetric stretching vibration of Si-O-Si of FA appeared at 1096 cm^{-1}. This Si-O-Si band shifted to the lower wave numbers of 934 cm^{-1} for 0AD geopolymer sample indicating the development of amorphous silicon aluminate gels [19]. The position of the functional group peaks depends on the bond lengths and angles, and shifts in the peaks indicate that reactions are occurring due to the formation of stronger new bonds. In the geopolymer samples made from fly ash with added aluminum dross residue, the peaks are consistent and similar across all samples, with only slight bond shifts to the higher wave number and variations in peak heights when the AD content increases.

3.7 Microstructure of geopolymer via FE-SEM

Fracture surface of the samples was investigated using FE-SEM technique as shown in Figure 11. The FE-SEM images revealed that there were some remained raw materials in all samples, for example, the spherical shape of fly ash particles was found in all samples. In Figure 11(a), the 0AD sample has fewer pores and smoother fracture surface. When AD was added (Figures 11(b-d), the fracture surface was found to be rough, uneven, and disconnected showing that these samples had more porosity.

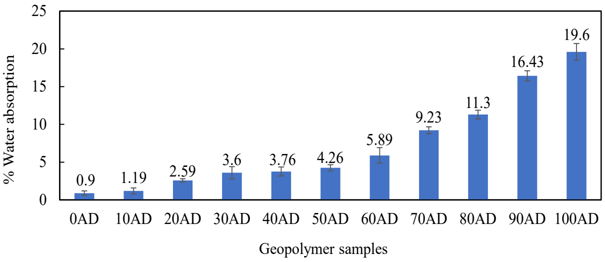

Figure 7. %Water absorption of geopolymer samples.

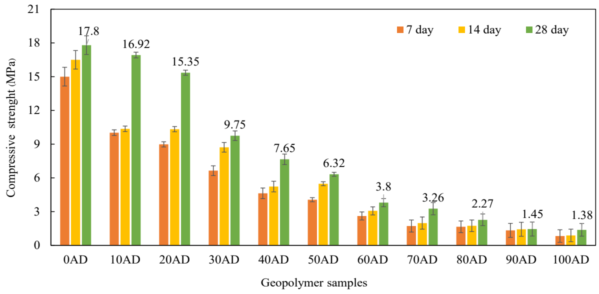

Figure 8. Compressive strength of geopolymer samples.

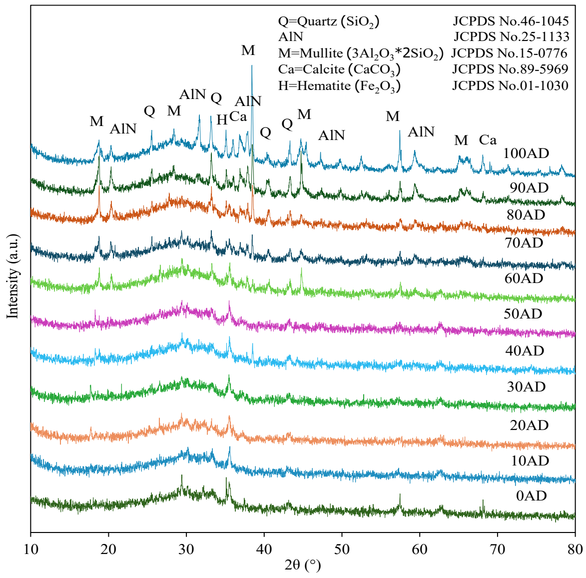

Figure 9. Phase structure of geopolymer samples.

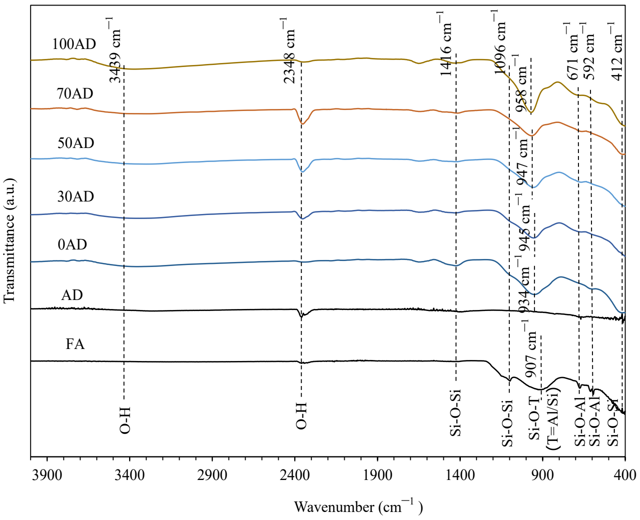

Figure 10. The chemical structure of the geopolymer samples.

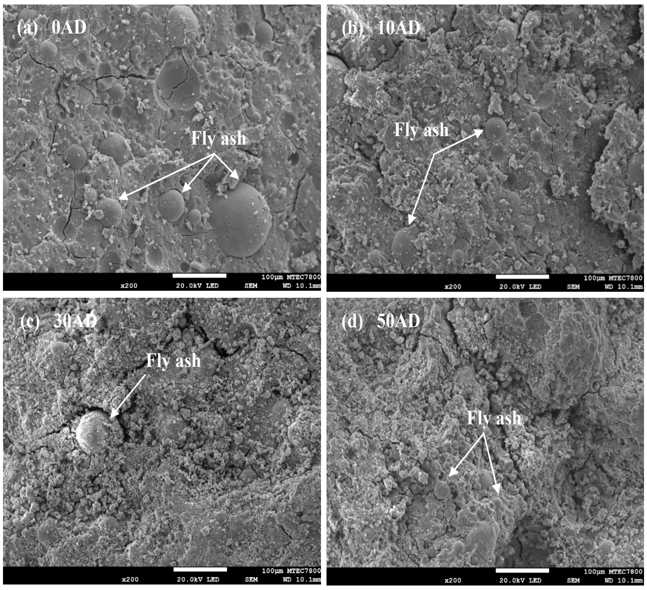

Figure 11. The microstructure of the geopolymer samples (a) 0AD, (b) 10AD, (c) 30AD, and (d) 50AD.

4. Conclusions

From the analysis results of the FA and AD based geopolymers, it was found that the reaction of AlN phase in AD with moisture or water during production led to the formation of ammonia gas bubbles. Once set, this resulted in a high porosity finished samples causing the low bulk density, high water absorption (%) and low compressive strength. On the other hand, the geopolymer samples containing 100 wt% FA has fast setting time with fewer pores, allowing them to withstand higher compression. However, too fast setting made the difficult forming process and poor workability. Thus, the addition of AD could retard the reaction and improve the forming behavior of the geopolymer products.

Amorphous phase found in XRD results of all samples indicated the geopolymer gel formation in the samples. However, there were some remained FA and AD raw materials in the geopolymer matrix as suggested by XRD and SEM results.

As suggested by the industry standards for lightweight concrete block products, TIS 2601-2013, it was found that the 50AD and 60AD samples could be suitable for use in this type of product because their properties remain within the ranges required in this construction application. It might be possible to enhance their mechanical properties further by adding fine aggregate or coarse aggregate. Finally, the present work shows that the AD can be used as the alternative raw materials for sustainable geopolymer products.

Acknowledgement

This work was supported by Thammasat University Research unit in Sustainable Materials and Circular Economy. The researchers would like to thanks the support of Top five manufactory Co., Ltd., the Electricity generating Authority of Thailand (Mae Moh Power Plant) and Mitrphol Bio-power Co., Ltd.

References

[1] W. Poonyakanok, "Green concrete," RISC.com. https://risc.in.th/th/knowledge/ (accessed Jan. 15, 2024)

[2] V. Shobeiri, B. Bennett, T. Xie, and P. Visintin, "A comprehensive assessment of the global warming potential of geopolymer concrete," *Journal of Cleaner Production*, vol. 297, p. 126669, 2021.

[3] F. N. Stafford, A. C. Dias, L. Arroja, J. A. Labrincha, and D. Hotza, "Life cycle assessment of the production of Portland cement: A Southern Europe case study," *Journal of Cleaner Production*, vol. 126, pp. 159-165, 2016.

[4] B. C. McLellan, R. P. Williams, J. Lay, A. van Riessen, and G. D. Corder, "Costs and carbon emissions for geopolymer pastes in comparison to ordinary portland cement," *Journal of Cleaner Production*, vol. 19, no. 9, pp. 1080-1090, 2011.

[5] H. Xu, and J. S. J. Van Deventer, "The geopolymerisation of alumino-silicate minerals," *International Journal of Mineral Processing*, vol. 59, no. 3, pp. 247-266, 2000.

[6] A. M. Rashad, "A comprehensive overview about the influence of different additives on the properties of alkali-activated slag – A guide for Civil Engineer," *Construction and Building Materials*, vol. 47, pp. 29-55, 2013.

[7] N. Toobpeng, P. Thavorniti, and S. Jiemsirilers, "Effect of additives on the setting time and compressive strength of activated high-calcium fly ash-based geopolymers," *Construction and Building Materials*, vol. 417, p. 135035, 2024.

[8] L. Zhang, Z. Chen, R. Chen, S. Zhu, J. Lin, and P. Tai, "Compressive strength of fly ash based geopolymer utilizing waste completely decomposed granite," *Case Studies in Construction Materials*, vol. 19, 2023, Art. no. e02667.

[9] M. Ashfaq, M. Sharif, M. Irfan-ul-Hassan, U. Sahar, U. Akmal, and A. Mohamed, "Up-scaling of fly ash-based geopolymer concrete to investigate the binary effect of locally available metakaolin with fly ash," *Heliyon*, vol. 10, 2024, Art. no. e26331.

[10] M. H. Elseknidy, A. Salmiaton, I. Nor Shafizah, and A. H. Saad, "A study on mechanical properties of concrete incorporating aluminum dross, fly ash, and quarry dust," *Sustainability*, vol. 12, no. 21, 2020.

[11] T. F. Choo, M. A. Mohd Salleh, K. Y. Kok, K. A. Matori, and S. Abdul Rashid, "Characterization of high-temperature hierarchical porous mullite washcoat synthesized using aluminum dross and coal fly ash," *Crystals*, vol. 10, no. 3, 2020.

[12] P. Puksisuwan, P. Laoratanakul, and B. Cherdhirunkorn, "Utilization of aluminium dross as a main raw material for synthesis of geopolymer," *Journal of Metals, Materials and Minerals*, vol. 27, no. 2, 2018.

[13] I. A Aziz, M. M. A. B. Abdullah, H. Yong, and L. Ming, "Behaviour changes of ground granulated blast furnace slag geopolymers at high temperature," A*dvances in Cement Research*, vol. 32, pp. 1-28, 2019.

[14] C. S. Thunuguntla, and T. D. Gunneswara Rao, "Effect of mix design parameters on mechanical and durability properties of alkali activated slag concrete," *Construction and Building Materials*, vol. 193, pp. 173-188, 2018.

[15] Industrial Scientific, "Understanding ammonia (NH_3) gas: risks, detection, and safety measures," https://www.indsci.com/en/blog/understanding-ammonia-nh3-gas-risks-detection safety-measures?form=MG0AV3 (accessed Mar 1, 2025)

[16] C. Freidin, "Cementless pressed blocks from waste products of coal-firing power station," *Construction and Building Material*s, vol. 21, no. 1, pp. 12-18, 2007.

[17] M. J. Mwiti, T. o. J. Karanja, and W. J. Muthengia, "Properties of activated blended cement containing high content of calcined clay," *Heliyon*, vol. 4, no. 8, 2018, Art. no. e00742.

[18] S. Lv, H. Ni, X. Wang, W. Ni, and W. Wu, "Effects of hydrolysis parameters on AlN content in aluminum dross and multi-variate nonlinear regression analysis," *Coatings*, vol. 12, no. 5, 2022.

[19] T. Mukhametkaliyev, M. H. Ali, V. Kutugin, O. Savinova, and V. Vereschagin, "Influence of mixing order on the synthesis of geopolymer concrete," *Polymers,* vol. 14, no. 21, 2022.